Particle-acceleration and radiation in the turbulent flow of a jet

K. Manolakou[1]**, A. Anastasiadis**[2]**, and L. Vlahos**[1]

[1] Section of Astrophysics, Astronomy and Mechanics, Department of Physics, University of Thessaloniki, GR-540 06 Thessaloniki, Greece
(manolaku; vlahos@astro.auth.gr)
[2] Institute of Ionoshperic and Space Research, National Observatory of Athens, Palea Penteli GR-152 36, Greece (anastasi@creator.space.noa.gr)

Abstract. We present a numerical model for electron acceleration and radiation inside the body of an extragalactic jet. We model the jet environment as a turbulent medium generating non-linear structures (eddies and/or shocks) through a cascading process. These structures act like in-situ accelerators for the electrons that are initially injected from the central engine. Two types of acceleration processes are considered: second order Fermi-acceleration and shock-drift acceleration, depending on the velocity of the turbulent eddies encountered.

We study the modulation of the energy distribution of electrons in such an environment, by incorporating synchrotron radiation losses in the time intervals between successive interactions of the particles with the turbulent structures. By performing a parametric study with respect to the level of turbulent activity and the time intervals between interactions, we calculate the temporal evolution of the cut-off frequency of the synchrotron radiation spectrum of the particles and discuss our results in connection with recent observations.

Key words: acceleration of particles – radiation mechanisms: non-thermal – shock waves – turbulence – galaxies: jets – radio continuum: galaxies

1. Introduction

Jets are one of the most spectacular manifestations of outflows appearing in such different physical systems as young stars or extragalactic sources. They are the channels through which mass, energy, momentum, and magnetic field are transported from the central region to the outer edges of a system. It is accepted by now that the radio emission of jets is due to synchrotron radiation from an ensemble of relativistic electrons (or e^+) embedded in a magnetic field (e.g. Begelman et al. 1984). In almost all cases the spectrum of the radiation can be fitted by one or the superposition of a number of power laws in frequency, ($F_\nu \sim \nu^{-\alpha}$), thus implying a power-law distribution for the emitting electrons ($dN \sim E^{-x}dE$). The index x is related to the spectral index α through the relation $x = 2\alpha + 1$. The values of α come in a surprising narrow range: $0.5 \leq \alpha \leq 1.0$, even

for different astrophysical systems. This yields for the particles' distribution index values $2.0 \leq x \leq 3.0$ (Scheuer 1984).

The linear dimensions of jets can reach values up to ~ 1 Mpc in some cases. Particles somehow seem to be able to maintain their high energies – otherwise lost due to synchrotron radiation losses – until very far from the central engine (Achterberg, 1986). In order to account for the observed radiation at such long distances, particles should be accelerated *in situ* (Felten 1968; Hargrave & Ryle 1974).

The few *bright knots*, which exist in the body of some jets, and are identified as regions of intense emission of radiation, are interpreted as *oblique shocks* moving down the jet (Bicknell & Begelman 1996). These shocks could act as in situ particle accelerators. Recent observational results, however, as those obtained by the synchrotron spectrum of the M 87 jet, led to the conclusion that the shocks associated with the bright knots cannot account for the acceleration. In addition, there are indications for permanent acceleration of the electrons even in the inter-knot regions. More specifically, Meisenheimer et al. (1996) showed evidence for astonishingly smooth variations of both the optical spectral index $\alpha_{\rm opt}$ and the radio-to-optical spectral index $\alpha_{\rm ro}$ along the jet axis of M 87.

There are a number of 2-D and 3-D numerical simulations studying the dynamical evolution and propagation of a hydrodynamic jet through the ambient medium and the evolution of the associated Kelvin-Helmholtz instabilities (Norman & Hardee 1988; Hardee & Norman 1989; Hardee et al. 1992; Hardee & Clarke 1992; Bodo et al. 1994, 1995; Hardee et al. 1995; Bassett & Woodward 1995). These numerical simulations give evidence for the formation of small-scale discontinuities in the form of shocks or vortices in the jet flow. Moreover, in the 3-D case, a very fast development of these structures is observed, caused either by the growth of linearly unstable, non-axisymmetric modes, or by the *non-linear cascade of energy* to smaller scales (Bodo et al. 1998).

The recent observations, as well as the numerical simulations suggest that the jet-environment may be more complex than it has been considered so far. This complexity might have a great impact on the acceleration process involved, as the existence of a turbulent flow could give a way of transferring some of the kinetic energy of the bulk flow to particle acceleration. The turbulent flow can generate local discontinuities throughout

---

Send offprint requests to: L.Vlahos

the jet, which may act as in situ particle accelerators (Pelletier & Zaninetti 1984).

Following the above scenario, we introduce a numerical model for permanent electron acceleration in a turbulent jet, where a particle's energy may vary due to collisions with small-scale structures (eddies) or/and encounters with shock fronts. In addition, particles are assumed to be subject to synchrotron losses during time intervals between successive interactions. Our goal is to study the influence of the jet environment on a power law energy distribution of electrons initially injected at the beginning of the jet. We construct a turbulent environment, which will be the generator of the turbulent structures which will act as accelerators for the particles. We calculate the final energy distribution of the particles and the corresponding synchrotron radiation spectrum, and perform a parametric study with respect to the level of turbulent activity and the time intervals between successive encounters. The evolution of the cut-off frequency as a function of time is also considered, and compared to the case of no in-situ acceleration, where only synchrotron losses are active.

This paper is organized as follows: In Sect. 2 we present our numerical model concerning the evolution of the turbulent environment, the acceleration processes involved, as well as the synchrotron radiation losses. Our results are reported in Sect. 3, followed by a summary and discussion in Sect. 4.

2. Model description

In this section, we present the general aspects of our model: We introduce the numerical model for the evolution of the turbulent environment, the acceleration processes, as well as the synchrotron radiation losses.

The values of the physical parameters of the jet are taken to be: $L = 1$ Mpc, $n_o = 10^{-4}$cm^{-3}, $B_o = 10^{-5}$G, and $T = 10^6$ K (Ferrari 1983). These are the linear dimension of the jet, the particle density of the medium, the magnetic field strength, and the temperature of the plasma, respectively. The corresponding value of the Alfven velocity is $V_A = 2.18 \times 10^8$ cm sec^{-1}. We assume that the flow velocity of the jet is non-relativistic and of the order $V_{jet} \approx 4V_A$. We also define the time $\tau \approx L/V_{jet} \sim 1.2 \times 10^8$ yrs as the minimum time for the transport of a turbulent structure from the beginning of the jet to the outer edge of the system.

2.1. The turbulent environment

According to Richardson's picture (Richardson 1922), turbulent motion consists in a large number of eddies (circular motions, whirlpools) of all kind of length scales, r, the biggest ones having sizes comparable with the size of the turbulent region, L. There is a cascade process of eddy breaking-down, in which there is a transmission of energy of the main flow to motions of smaller and smaller eddies down to the length scale, η, where the fragmentation process is stopped and the energy is dissipated. The range of length scales, r, for which $L \gg r \gg \eta$ is called the inertial subrange of fully developed turbulence.

According to the theory of Kolmogorov (1941a; 1941b) – which stated that the mean energy dissipation rate (transmitted energy per kilogram per second), ϵ is constant – the velocity differences in a turbulent velocity field separated by a distance r should display a simple scaling behavior, that is $\Delta u(r) \sim r^{1/3}$. Thus the structure function, $S(r,p)$ (the velocity differences raised to the p power), should scale as $\sim r^{p/3}$. Experimental results however (e.g. Anselmet et al. 1984) showed that $S(r,p) \sim r^{\zeta(p)}$, where $\zeta(p)$ deviates from the classical Kolmogorov value $p/3$ for $p < 3$ and $p > 3$.

The basic weakness of Kolmogorov's prediction was due to the assumptions that turbulence is space-filling and homogeneous. Instead, the real picture (see for e.g. Frisch & Morf 1981) shows that turbulence is highly intermittent and strongly inhomogeneous: short durations of almost zero velocity are alternated by strong velocity bursts of different strength, thereby suggesting that different eddies of size r carry different amounts of energy. Thus, fractal theory initially (Novikov & Steward 1964; Mandelbrot 1974; Frisch et al. 1978) and then multifractal theory (Parisi & Frisch 1985) were invoked in order to take into account the aspects of intermittency and both intermittency and inhomogeneity in turbulence, respectively.

These aspects (intermittency and inhomogeneity) of turbulence are very important for our model, as the sudden appearance of superalfvenic velocity eddies will result in the formation of shock waves, which greatly enhance the acceleration efficiency.

A number of fractal and multifractal models for hydrodynamic turbulence have been developed in the past years based on Richardson's energy-cascade picture (Frisch & Parisi 1984; Frisch et al. 1978; She & Leveque 1994). As experimental measurements of the probability densities of multiplier distributions (Novikov 1971; Van Atta & Yeh 1973) became more accurate (Chhabra & Sreenivasan 1992), some of these models (Menneveau & Sreenivasan 1987; Benzi et al. 1984) turned out to be simplifications of the actual dynamical process. Their biggest omission being that they do not display the correct local as well as global scaling behavior (i.e. the multiplier distributions deviate from the experimental ones (Chhabra & Sreenivasan 1992)).

In order to simulate the turbulent flow inside the jet we use the Simple Stochastic Selfsimilar Branching (SSSB) model introduced by Kluiving & Pasmanter (1996). This seems to be one of the most successful models. It describes Richardson's energy flux cascade for inertial subrange turbulence. It is a one-dimensional, stochastic, multifractal cascade-model, mimicking the break-up of structures along a one-dimensional cut through the isotropic turbulent velocity field. A structure has two possibilities: it either branches into two daughters with probability $(1 - P)$, or it does not branch, with probability P.

If an eddy brakes into one daughter (unbrakes) then this eddy will have size r_o times the size of the mother eddy and the same energy flux (the energy in a domain r, that is transferred per second to smaller length scales) as the mother eddy. If it brakes into two daughters, then one of them has size r_1 times the size of the mother eddy and energy flux p_1 times the energy flux of the mother eddy, while the other daughter has size r_2 times the size of the mother eddy and energy flux $(1 - p_1)$ times

the energy flux of the mother eddy. Thus the model comprises five free parameters: P, r_o, r_1, r_2 and p_1.

This process is recursively repeated for each daughter. The value of repetition of the process is called *the stage of construction* of the environment (for e.g. if the stage of evolution is 20 the process has been repeated for 20 successive times). In this way, the energy of the initial structure is transferred to smaller and smaller scales, up to the smallest scale where it is dissipated.

The basic advantages that the SSSB model combines compared to other cascade models mentioned above are the following:

i)   it is a multifractal model, that means it takes into account both intermittency and inhomogeneity in constructing the energy flux cascade,
ii) the total energy flux is conserved in the scales $L \gg r \gg \eta$,
iii) For only one non trivial set of values for the above five parameters:
   (a) the multiplier distributions that are calculated from the model are close to the experimental ones. Also the $D(q)$ multifractal spectrum is in very good agreement with the observations,
   (b) the energy flux probability densities along different inertial-subrange length scales, r, show square root exponential tails, in agreement with the corresponding experimental ones.

This model provides the energy dissipation rate as a function of the internal subrange of turbulence ($\epsilon(r)$). From that we calculate the velocity of the eddies $V(r)$ using the 2nd refined hypothesis introduced by Kolmogorov (1962):

$$V(r) \sim [r\epsilon(r)]^{1/3}. \tag{1}$$

The above velocity spectrum is normalized in a way, so that the maximum eddy velocity is equal to V_{jet}. The direction of motion of the eddies is randomly selected to be either in the direction of the jet flow or opposite to it.

We use this environment to accelerate electrons via two types of acceleration mechanisms: the second order Fermi mechanism and the shock drift mechanism. For both cases the eddies act as accelerators. We introduce a threshold in the value of the velocity of the eddies, $V_{\text{thr}} = 1.5V_A$, above which the shock mechanism is applied, otherwise Fermi acceleration is taking place. The reason is that the higher velocity structures (eddies) create discontinuities of larger sizes as they compress effectively the ambient flow locally. Thus we assume that the higher velocity eddies produced by the SSSB model introduce shocks in the jet flow.

2.2. The acceleration processes

As an electron moves inside the jet flow it encounters both the above mentioned discontinuities (eddies and/or shocks). If the electron interacts with a structure with velocity $V < V_{\text{thr}}$, it changes its energy according to the **second order Fermi mech-**

anism (Fermi, 1949; 1954). The increment of the total energy of the particle is given by the relation (Longair, 1983):

$$\Delta E = \pm 2\gamma^2 E_1 V(u \pm V)/c^2 \tag{2}$$

where γ is the Lorentz factor: $\gamma = [1 - (V/c)^2]^{-1/2}$, u and E_1 are the velocity and the total energy of the particle before the collision and c is the velocity of light. The plus (minus) sign stands for head-on (following) collisions of the electrons with eddies. From Eq. 2, it is evident that an electron can be accelerated or decelerated depending on the direction of the encounter.

In the case that an electron interacts with a structure having velocity $V \geq V_{\text{thr}}$, it undergoes acceleration by a shock front. Particles can in general be accelerated in shock waves by either the *drift* or the *diffusive* acceleration mechanism (for a review see Jones & Ellison 1991). In the case of the diffusive mechanism, a particle is accelerated as it scatters many times back and forth across the shock front off magnetic irregularities which exist in the upstream and downstream region (Drury 1983; Scholer 1985). In the drift mechanism, a particle gains energy as it drifts along the electric field at the shock front (Sarris & Van Allen 1974; Armstrong et al. 1985; Decker 1988). In this case, a particle interacts only once with the shock front and never returns to it. When turbulence is present upstream and downstream of an oblique shock wave, particles can be accelerated by a combination of the drift and the diffusive mechanism (Decker & Vlahos, 1986).

Several applications of the diffusive shock acceleration mechanism of energetic electrons subject to synchrotron losses have been made, using a transport equation of particles, in order to explain the observed radiation spectrum of extragalactic radio sources (Heavens & Meisenheimer 1987; Fritz 1989; Blackman 1996). A number of models involving also diffusive shock acceleration by an ensemble of shock waves have been proposed (Achterberg 1990; Schneider 1993; Pope et al. 1996).

Begelman & Kirk (1990) applied the drift acceleration mechanism for the case of a superluminal oblique shock wave, in order to model the compact hot spots of extragalactic radio sources. Anastasiadis & Vlahos (1993) considered the case of multiple shock acceleration using the shock drift mechanism in order to explain the emitted radiation spectrum from the hot spots. Based on this model, we consider here the case of the **shock drift acceleration mechanism**. We apply this specific mechanism because we are able to calculate analytically the energy change of the electrons during the interaction using the adiabatic treatment (for details see Decker 1988).

For each shock front we assume that the upstream plasma values are: $U_1 = V$, $1.5 \leq M_{A_1} \leq 4.0$, $20^o \leq \theta_{Bn_1} \leq 60^o$, $B_1 = 10^{-5}$ G and $\beta_1 = 0.35$, where U_1 is the plasma flow velocity, $M_{A_1} = U_1/V_A$ is the Alfvenic Mach number, θ_{Bn_1} is the angle between the shock normal and the direction of the upstream magnetic filed B_1, and β_1 is the plasma parameter beta. The angle θ_{Bn_1} is chosen randomly from the above given range, while the Alfvenic Mach number is provided by the model for the environment we have used (SSSB model). We evaluate the downstream plasma parameters from the upstream ones using

the MHD jump conditions known as *Rankine-Hugoniot* conditions (Tidman & Krall 1971).

We consider only the case of those electrons which before the shock encounter are upstream of the shock front and are transmitted into the downstream region after the shock encounter. We do not follow the evolution of the pitch angle at the end of each electron-shock encounter. This assumption is based on the random choice of the parameters that govern the acceleration mechanism (e.g. θ_{Bn}, M_{A_1}). The kinetic energy, T_2, of the downstream transmitted electrons, is given by the relation (Decker 1988):

$$\frac{T_2}{T_1} = 1 + \gamma_1(\gamma_1 - 1)^{-1}\beta_1 R_1 \{ \frac{1}{2}(1 + f^2)\varepsilon_1$$
$$+\mu_1 - f[(\varepsilon_1 + \mu_1)^2 - (b-1)(1 - \mu_1{}^2)]^{1/2} \}, \qquad (3)$$

where γ is the Lorentz factor of an electron, $\beta = u/c$ (u is the electron's velocity), μ is the cosine of the electron's pitch angle, $b = B_2/B_1$ is the ratio of the downstream to upstream magnetic field, r is the compression ratio of the shock wave, $f = b/r$, $R = V \sec\theta_{Bn}/c$ and $\varepsilon = Rc/u$. Finally, we must state here that the subscripts 1 and 2 stand for the upstream and downstream regions of a shock front, respectively.

Summarizing, we conclude that as the electron travels it encounters both kinds of discontinuities: eddies and shocks, depending on the velocity of the latter: if an electron interacts with a turbulent eddy with velocity $V < V_{thr}$, then the second order Fermi mechanism is applied and the increment in the energy of the electron is given by Eq. 2. Similarly, if an electron interacts with a shock wave with velocity $V > V_{thr}$, the shock-drift mechanism is applied, the electron is transmitted downstream and the new value in its energy is given by Eq. 4.

2.3. The radiation losses

In addition to the acceleration processes described above, we include synchrotron radiation losses for the electrons during the time intervals between successive interactions with the turbulent structures.

The mean energy change of an electron (in erg) due to synchrotron radiation is given, assuming isotropic pitch angle distribution, by the relation (see Pacholczyk 1970):

$$\langle \Delta E_j \rangle = -2.36 \times 10^{-3} B_o^2 \{(1 - \frac{1}{3}\beta_j{}^2)E_j{}^2 - E_o{}^2\}T_j, \qquad (4)$$

where E_j is the energy of the electron after the jth interaction with an eddy, E_o is the rest mass energy of the electron, β_j is the electron's velocity normalized with the speed of light, B_o is the ambient magnetic field in Gauss and T_j is the time interval in sec between the jth and the (j+1)th interaction. We must emphasize that the acceleration of electrons is a localized process in our model, but the losses due to synchrotron radiation are active continuously along the trajectories of the electrons and play a very important role for the formation of their final energy distribution.

Table 1. The three cases (T_1, T_2 and T_3, respectively) we study for the time intervals, T, between successive interactions of the electrons with the turbulent structures (eddies). Columns from left to right: T_{min}, T_{max}: the minimum and maximum value for the time intervals; $\langle T \rangle$: the corresponding mean value.

Case:	$T_{min} - T_{max}$ (yrs)	$\langle T \rangle$ (yrs)
T_1:	$10^5 - 5 \times 10^5$	$\sim 2.5 \times 10^5$
T_2:	$10^2 - 10^5$	$\sim 5 \times 10^4$
T_3:	$10^2 - 10^4$	10^3

3. Numerical results

In this section we present the results of the model presented above. We perform a parametric study on the modulation of an initial power-law energy-distribution of electrons injected at the beginning of the turbulent jet, and calculate the corresponding synchrotron radiation spectrum after time $\sim \tau$. In addition, the temporal evolution of the cut-off frequency is calculated for the same time $\sim \tau$ and compared to the case where only synchrotron losses are active along the electrons' trajectories.

The free parameters of our model are (1) the level of turbulent activity of the jet flow, and (2) the time intervals between successive interactions of the electrons with the turbulent structures (eddies and/or shocks). As we mentioned before, the level of turbulent activity is governed by an external parameter of the SSSB model called the stage of construction (see Kluiving & Pasmanter 1996). We have chosen two different cases. In the first case (environment A), the stage of evolution is taken to be between a narrow range of small values, that is, between 20 and 30. In the second case (environment B), the range is larger taking values between 10 and 80.

The case of environment A corresponds to the region of the formation of the eddies, which is considered to be near the boundary layer of the jet, where the bigger (mother) eddies are expected to form. On the other hand, environment B corresponds to a more inner zone, where the smaller scale structures are more dominant due to the cascading process of the bigger eddies from the boundary layer.

The time interval, T, between successive interactions of particles with the turbulent structures is the other important parameter of our model, as it influences the energy distribution of particles through the synchrotron radiation losses. These time intervals (T) are chosen randomly from T_{min} to T_{max}. We have studied three distinct cases by varying the two above limits (T_{min} to T_{max}) and consequently varying the mean value of the time intervals, $\langle T \rangle$.

We must emphasize that the duration of the modulation of the injected distribution through the turbulent environment must be of the order of $\tau \approx 10^8$ yrs. It is clear then, that the random choice of T is closely connected to the mean number of encounters that the particles will undergo with the structures. In Table 1, we give the upper and lower values as well as the mean values of the time intervals, for the three cases studied here (T_1, T_2 and T_3, respectively).
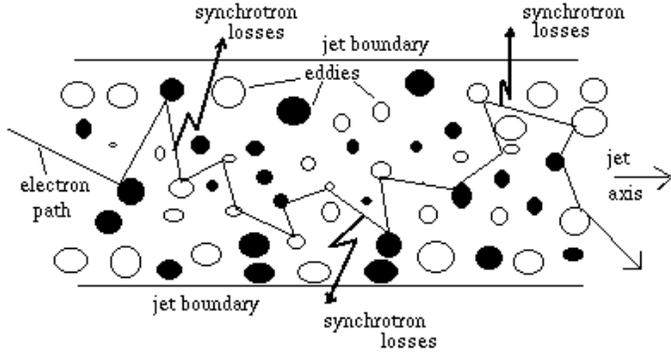
Fig. 1. A cut along the jet axis illustrating the acceleration model. The continuous line represents the trajectory of an electron. The black and white circles represent turbulent eddies encountered by the electrons. After an encountered with a black (white) eddy the electron looses (gains) energy. The electron, also looses energy between successive interactions, due to synchrotron radiation losses. The bigger eddies are formed close to the boundaries of the jet, due to its interaction with the ambient medium (environment A). In the more inner zone the eddies become smaller and smaller due to the cascading process (environment B).

Fig. 3. The same as Fig. 2, but for the case of environment B.

Fig. 2. The velocity time series of the structures produced by the SSSB model, for the case of environment A, as seen by an electron moving random travel times T_1. The dashed lines correspond to the threshold velocity, $|V_{\mathrm{thr}}| = 3.27 \times 10^8$ cm/sec.
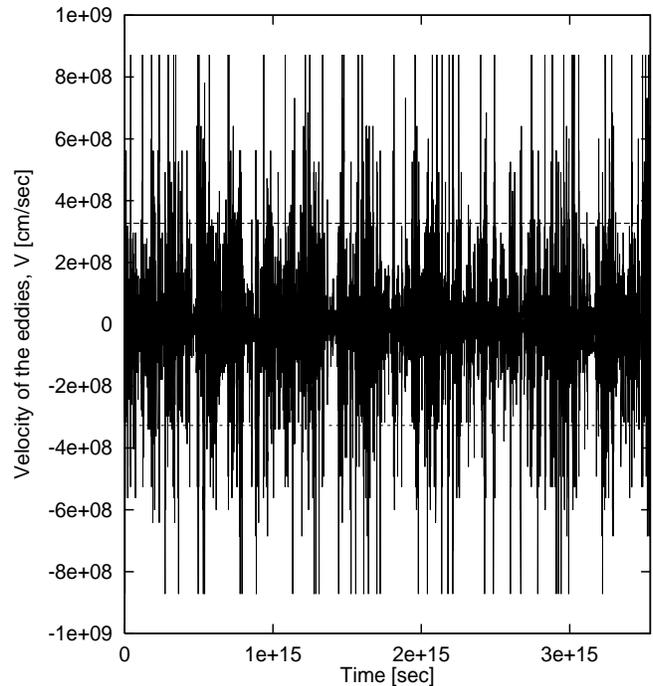
Fig. 4. The same as Fig. 2, but for the case T_3.

In Fig. 1 we present an illustration of the electron acceleration model.

First, we will report our results concerning the development of the turbulent environment. In Figs. 2 and 3 we present the velocities of the eddies in environment A and B, respectively, as seen by an electron along its path for the T_1 case. Similarly, in Figs. 4 and 5 we present the corresponding velocity time series
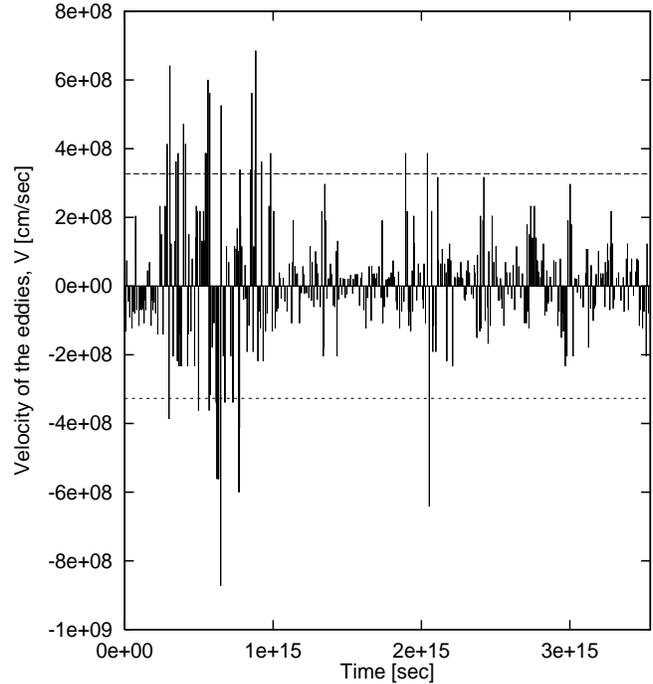
for the case of T_3. The velocity profiles of T_2-case lie between the two above cases.

It is obvious that for small $\langle T \rangle$ the electron undergoes a larger number of interactions with structures. As the level of turbulent activity is low (environment A) and $\langle T \rangle$ is small, the number of shocks (structures with $V \geq V_{\mathrm{thr}}$) encountered by the particle is larger than the corresponding one in environment B
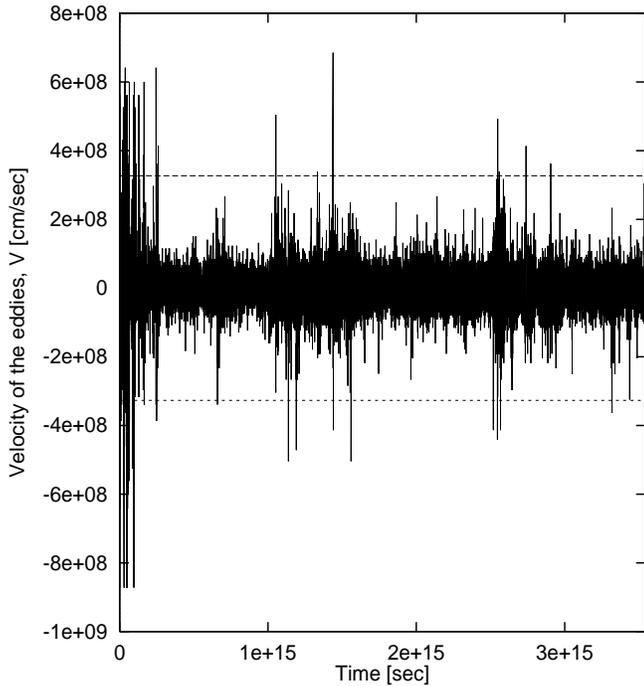
Fig. 5. The same as Fig. 4, but for the case of environment B.

(see Figs. 4 and 5). On the other hand, when $\langle T \rangle$ becomes bigger the particles undergo less interactions and the number of shocks encountered is more or less the same for both environments (see Figs. 2 and 3).

In Fig. 6, the temporal evolution of the normalized mean energy for an initially monoenergetic population of $N = 20000$ electrons interacting with environment A and B, respectively, is presented. Particles are injected with initial energy $E = 10.5$ MeV at the beginning of the jet, and the range of the time intervals is $10^2 \leq T \leq 10^4$ yrs (case T_3). In order to investigate the influence of synchrotron losses on the evolution of the particles' energy, we present the cases with and without synchrotron losses.

We note that the environment A is a more efficient accelerator than the environment B, even when synchrotron losses are acting along the trajectories of the electrons. In the case where no synchrotron losses are included, the small fluctuations of the mean energy of the particles are due to the stochastic nature of the acceleration mechanisms involved (see Fig. 6).

We study next the case that the injected energy distribution of the particles is a power law with index $s = 2.0$ and $s = 3.0$ in the energy range 10^7 eV $\leq E < 10^{11}$ eV. It turns out that for all three cases T_1, T_2 and T_3, both for environment A and B, the final energy distribution has also a power-law form:

$$dN_f(E) \propto K E^{-x} dE \qquad (5)$$

where K is a constant. Moreover, the value of the index x is very close to the value of the injected index, s. The numerical fittings of the final distributions were tested by a χ^2-test and found to be acceptable on a 95% significance level. In Fig. 7 we present the results regarding the final energy distribution of electrons for the case T_3, power-law injection with index

$s = 2.0$ and environments A and B, ((a) and (b) in Fig. 7) respectively. We have chosen to present the T_3-case here, since for the corresponding value of the time intervals the highest value of the maximum energy is achieved. Also shown is the case were only synchrotron losses are included ((c) in Fig. 7). As we have already mentioned, the slope of the power law remains very close to its initial (injected) value, similarly to the case where only synchrotron losses are active. Looking at the maximum energies obtained for the three cases ((a), (b) and (c)), we see that the acceleration model (for both environment A and B) is able to sustain electrons with high energies. These electrons don't appear in the case where only synchrotron losses are active (case (c)), as they have radiated away their energies.

Furthermore, we calculate the intensity of the radiated power as a function of frequency using the formula (De Young 1984):

$$I(\nu) \sim \frac{\sqrt{3}}{4\pi(x+1)}\Gamma\Big(\frac{3x-1}{12}\Big)\Gamma\Big(\frac{3x+19}{12}\Big)\frac{e^3}{mc^2}$$
$$\Big(\frac{3e}{2\pi m^3 c^5}\Big)^{(x-1)/2} K B_o^{(x+1)/2}\nu^{-(x-1)/2}, \qquad (6)$$

where Γ is the Euler gamma function, B_o is the ambient magnetic field, K and x are given in Eq. 5, and ν is the frequency. In Fig. 8 we plot the intensity as a function of frequency corresponding to the final distributions (see Fig. 7) of a power-law injection with index $s = 2.0$, for the T_3-case and for both environments (A and B). From Fig. 8 we can see that the maximum frequency, with emission which corresponds to the cut-off frequency, is higher for environment A. As mentioned before, this is due to the fact that environment A is a more efficient accelerator than environment B. The spectral index α ($\alpha = (x-1)/2$) is of the order of $\alpha \sim 0.5$, for $x \sim 2.0$ ($s = 2.0$), and for $x = 3.0$, $\alpha \sim 1.0$ ($s = 3.0$).

In Fig. 9 we present the evolution of the cut-off frequency, ν_c, as a function of time, t, for the T_3-case of environment A ($s = 2.0$). Also shown is the theoretically calculated curve for the time evolution of the cut-off frequency by means of Eq. 4 and the formula (Melrose, 1980):

$$\nu \sim 5 \times 10^{-6} E_{eV}^2 B_o \qquad [Hz] \qquad (7)$$

where ν is the mean frequency radiated by an electron and E_{eV} is the total energy of the electron in eV units. By using $E = E_{max}$, we derive the cut-off frequency, $\nu = \nu_c$. The numerically calculated temporal evolution of the cut-off frequency (curve (a) in Fig. 9) was performed by estimating the time evolution of the initially injected power-law distribution, as it is transported down the jet. It turned out that the power-law form of the electron energy distribution (equivalently of the radiation spectrum) is preserved as we move down the jet.

From Fig. 9 we also see that the cut-off frequency deduced from the acceleration model (environment A) is *always* higher than the corresponding value of the cases where only synchrotron losses are active in the trajectories of the electrons. For $t \sim \tau$ we have $\Delta\nu_c \sim 100$ MHz That means that the model is able to preserve a part of the spectrum even at large distances (down the jet). We wouldn't be able to observe this part of the
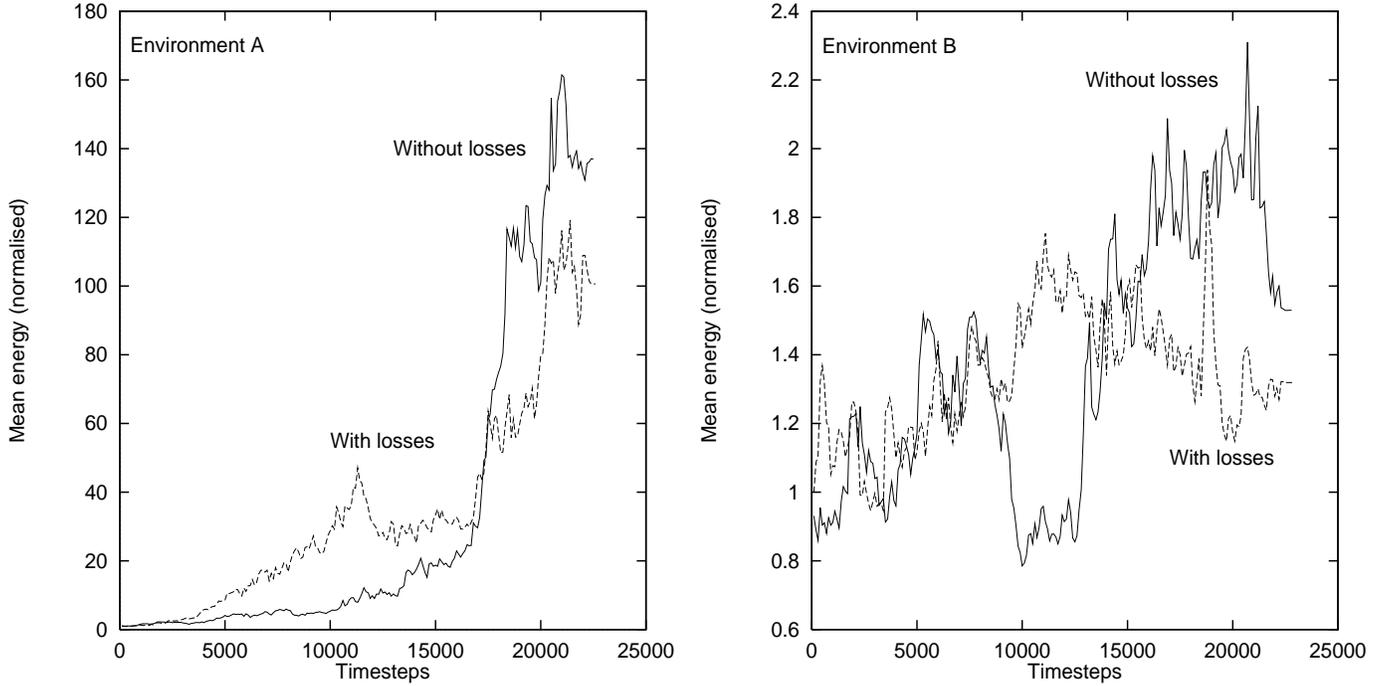
Fig. 6. The time evolution of the mean energy of $N = 20000$ monoenergetic particles moving with random timesteps between $T_{\min} = 10^2$ and $T_{\max} = 10^4$ yrs, for the cases of the environment A (left panel) and B (right panel), respectively. In the upper curves no synchrotron radiation losses are included, opposite to the lower curves.
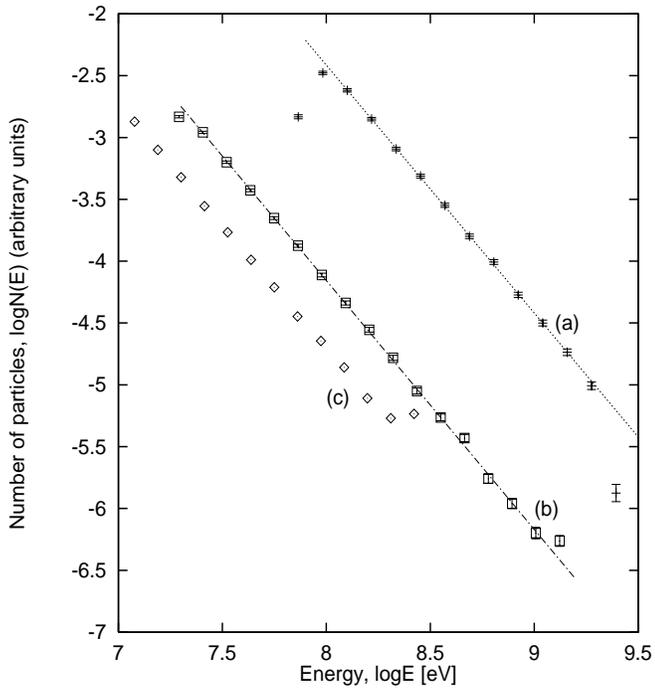

Fig. 7. The final energy distribution function of a total number of 20000 particles injected at the beginning of the jet, for the case of $T_{\min} = 10^2$ and $T_{\max} = 10^4$ yrs ($s = 2.0$). Curve a (b) corresponds to the case of the environment A (B), while c stands for the case that only synchrotron losses are active.
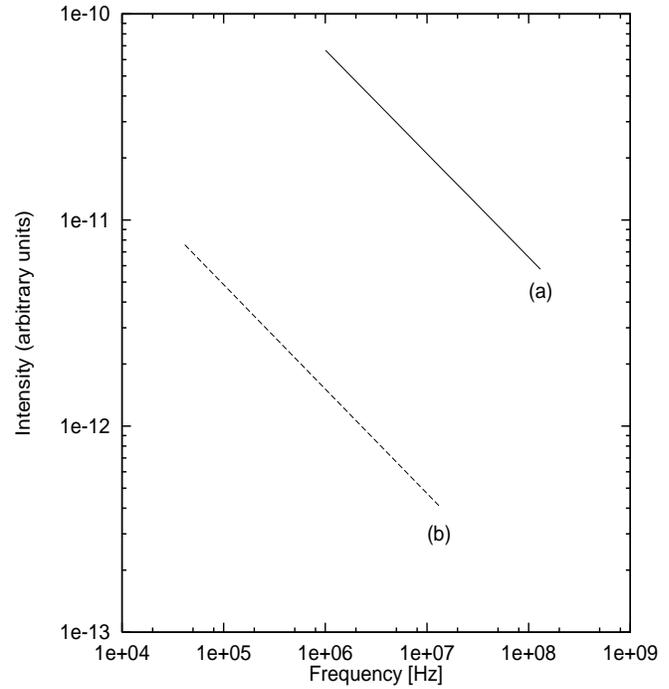
Fig. 8. The intensity of the emitted radiation as a function of frequency for the case of $T_{\min} = 10^2$ and $T_{\max} = 10^4$ yrs ($s = 2.0$). The curve (a) corresponds to the case A, and (b) to the case of environment B.

spectrum without in-situ acceleration due to synchrotron cooling of the particles.

Another external parameter of our model is the value of the threshold velocity, V_{thr}. The value of the threshold velocity is defined essentially through the lower value of the velocity of
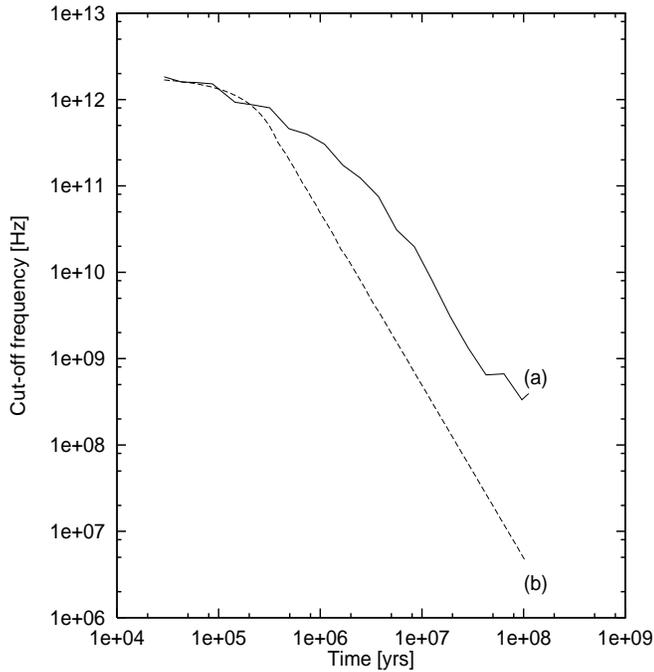
Fig. 9. The cut-off frequency of the emitted radiation as a function of time, for the T_3-case of environment A ($s = 2.0$). The continuous curve (a) corresponds to the case of environment A, while the dashed one (b) to the case where only synchrotron losses are included in the model.

shock waves. The velocities of the shock waves, V, used here ly in the range $V_A < V \leq 4V_A$ (superalfvenic shocks). Due to the high intermittency of the velocity field and in order to have a sufficient number of shock waves, we have taken the value of the threshold velocity to be of the order of $1.5V_A$. This parameter does not change the form of the distribution of the electrons, but contributes only to the efficiency of the process. Indeed, by raising its value (for e.g. $V_{thr} = 2.5V_A$), we lower the number of shocks encountered by the electrons (see Figs. 2-5), thus rendering the process less efficient.

4. Summary and discussion

We have introduced a one dimensional numerical model for permanent acceleration and radiation of electrons in extragalactic jets. We have modeled the non-relativistic flow inside the body of a jet as a turbulent one, able to produce eddies depending upon the level of activity. These structures accelerate electrons via second order Fermi acceleration or shock drift acceleration. If the velocity of the structures (eddies) encountered by the particles is less than a threshold value (V_{thr}), the former acceleration mechanism is applied (see Eq. 2), otherwise the latter one (see Eq. 4). Thus the acceleration mechanismed used here is a mixed one.

Synchrotron losses (see Eq. 4) were included between the successive interactions of the electrons with the turbulent structures. The study of the time evolution of the mean energy of a monoenergetic distribution of electrons (see Fig. 6) shows that these losses play an important role in the evolution of the parti-

cles' energy as they are continuously active along the trajectory of the electrons, while the acceleration is a localized process.

Concerning the final energy distribution of the injected electrons, as well as the corresponding spectrum of the emitted radiation we have performed a parametric study with two free parameters: (1) the level of turbulent activity in the jet flow, and (2) the time intervals between successive interactions of the electrons with the turbulent structures.

The level of turbulent activity is governed by an external parameter of the SSSB model called the "stage of construction". The stage of construction is the value of repetition of the cascading process through the specific cascade model we have used. The lower the stage of construction the lower the level of turbulent activity. We have chosen two distinct cases. In the first one, the stage of construction of the environment is taken to lie in a narrow range of small values. In the second case, the range is larger. An environment with lower levels of turbulent activity is appropriate for describing the conditions in the boundaries of a jet, where bigger structures (eddies) are expected to form, while one with higher levels of turbulent activity is appropriate for a more inner zone, where smaller scale structures are dominant, due to the cascading process of the bigger eddies in the boundary layer.

The time intervals between successive interactions of the particles with the eddies are chosen randomly out of a certain range (Table 1). The mean value of these time intervals is closely related to the mean number of encounters of the particles with turbulent structures.

The value of the threshold velocity, essentially determines the number of shocks encountered by the electrons. By raising (decreasing) this value we lower (increase) the number of shocks and raise (decrease) the number of eddies encountered by the electrons, respectively. This fact does not change the form of the electron distribution, but it affects the efficiency of the process. For example, by raising (lowering) the threshold velocity, the maximum energy of the electrons' energy distribution is decreasing (increasing).

In the case that the injected distribution is of a power-law form ($s = 2.0$ or 3.0), we find that the final distribution is also of power-law form. The value of the index, x, of the final energy distribution of the particles is very close to the injected one (s). Also the index of electron distribution shows minor fluctuations throughout the jet corresponding to an almost steady value of the index α of the radiation spectrum.

Thus, for power-law injection with $s = 2.0$, we get $\alpha \sim 0.5$, both for environment A and B (cases T_1, T_2 and T_3). This result is in good agreement with observational results of the radio spectral index of jets, which give values of the order of $\alpha_r = 0.5$ (e.g. Meisenheimer et al. (1996)). Also, the fact that corresponding spectral indices for environment A and B are very close is consistent with the observations that the radiation indices, in radio wavelengths, across a jet are almost constant (e.g. in a section normal to the jet axis; Meisenheimer et al. (1996)).

The higher value for the maximum energy in the distribution of the electrons is achieved for the T_3-case and environment A.

We should add here though, that even for this case the maximum energy achieved is approximately half an order of a magnitude less than the maximum energy of the injected energy electron distribution. It seems that there is a balance between the energy losses and gains of the electrons, which follow from the mixed acceleration mechanism we used as well as the influence of the synchrotron radiation losses. This stands for the biggest part of the injected energy spectrum, but not for the upper part, since in high energies the synchrotron radiation losses become dominant, while the acceleration processes involved do not contribute enough to compensate for the losses.

Concluding, we might say that the level of turbulent activity has minor or no impact on the spectral index α, but contributes only to the efficiency of the acceleration process. The initial levels of activity (environment A) are more efficient in transferring a part of the energy of the bulk flow into kinetic energy of turbulent motions (eddies), which in turn act as more efficient accelerators for the particles. On the other hand, as the level of turbulent activity increases (environment B), the eddies tend to be smaller and slower, thus transferring less energy to the incident particles through collisions.

Our results show that special attention should be drawn to the characteristics of the jet as an environment, because they can play a very important role in the formation and modulation of the energy distribution of particles that are injected from the central object.

Nevertheless, our model exhibits some important drawbacks. First of all, we must state that there is no evidence for the formation of a power-law energy distribution in the beginning of the jet, close to the central object. Also, the model is capable of sustaining only a part of the electron energies that are injected initially (see Fig. 9). Moreover, the higher value of the maximum energy achieved by the model is derived using a certain range of the input parameters (T_3-case, environment A), but still is approximately half an order of magnitude lower than the corresponding value of the injected distribution.

In our opinion, more attention should be paid in the acceleration mechanisms used here. The Fermi acceleration mechanism proved inadequate in accelerating electrons in energies high enough to account for the radiation losses, as well as the the observations of the radiation spectrum of the jets in higher frequencies ($\nu > 1$ GHz). The choice of shock acceleration mechanisms (e.g. shock drift and diffusive shock acceleration) acting exclusively in the jet, might give a better approach to the problem.

References

Achterberg A., 1986, Particle Acceleration in Astrophysical Jets. In: W. Kundt (ed.) NATO ASI Series, vol. C 208, Astrophysical Jets and their Engines. Reidel, Dordrecht, p. 223

Achterberg A., 1990, A&A 231, 251

Anastasiadis A., Vlahos L., 1993, A&A 275, 432

Anselmet F., Gagne Y., Hopfinger E.J., Antonia R.A., 1984, J. Fluid Mech. 140, 63

Armstrong T.P., Pesses M.E., Decker R.B., 1985, Shock Drift Acceleration. In: Tsurutani B.T., Stone R.G. (eds.) Geoph. Mongr. Ser., 35, p. 271 Collisionless Shocks in the Heliosphere: Reviews of Current Research

Bassett G.M., Woodward P.R., 1995, ApJ 441, 582

Begelman M.C., Blandford R.D., Rees M.J., 1984, Rev. Mod. Phys 56, 255

Begelman M.C., Kirk G.J., 1990, ApJ 353, 66

Benzi R., Paladin G., Parisi G., Vulpiani A., 1984, J. Phys. A 17, 3521

Bicknell G.V., Begelman M.C., 1996, ApJ 467, 597

Blackman E.G., 1996, ApJ 456, L87

Bodo G., Massaglia S., Ferrari A., Trussoni E., 1994, A&A 283, 655

Bodo G., Massaglia S., Rossi P., et al., 1995, A&A 303, 281

Bodo G., Rossi P., Massaglia S., et al., 1998, A&A 333, 1117

Chhabra A.B., Sreenivasan K.R., 1992, Phys. Rev. Lett. 68, 2762

De Young D.S., 1984, Phys. Rep. 111, No 6, 373

Decker R.B., 1988, Space Sci. Rev. 48, 195

Decker R.B., Vlahos L., 1986, ApJ 306, 710

Drury L.O'C., 1983, Rep. Prog. Phys. 46, 973

Felten J.E., 1968, ApJ 151, 861

Ferrari A., 1983, In: Kundu M.R., Holman G.D. (eds.) IAU Symposium No 107, Unstable Current Systems and Plasma Instabilities in Astrophysics. Reidel, Dordrecht, p. 393

Fermi E., 1949, Phys. Rev. 49, 1169

Fermi E., 1954, ApJ 119, 1

Frisch U., Morf R., 1981, Phys. Rev. A, 23, 2673

Frisch U., Parisi G., 1984, In: Gil M., Benzi R., Parisi G. (eds.) Turbulence and Predictability in Geophysical Fluid Dynamics. North-Holland, Amsterdam

Frisch U., Sulem P.L., Nelkin M., 1978, J. Fluid Mech. 87, 719

Fritz K.D., 1989, A&A 214, 14

Heavens A.F., Meisenheimer K., 1987, MNRAS 225, 335

Hardee P.E., Clarke D.A., 1992, ApJ 400, L9

Hardee P.E., Clarke D.A., Howell D.A., 1995, ApJ 441, 644

Hardee P.E., Cooper M.A., Norman M.L., Stone J.M., 1992, ApJ 399, 478

Hardee P.E., Norman M.L., 1989, ApJ 342, 680

Hargrave P.J., Ryle M., 1974, MNRAS 166, 305

Jones F.C., Ellison D.C., 1991, Space Sci. Rev. 58, 259

Kluiving R., Pasmanter R.A., 1996, Phys. A 228, 273

Kolmogorov A.N., 1941a, Doklady Akademii Nauk SSSR, 30, 301

Kolmogorov A.N., 1941b, Doklady Akademii Nauk SSSR, 32, 16

Kolmogorov A.N., 1962, J. Fluid Mech. 13, 82

Longair M.S, 1983, High Energy Astrophysics. Cambridge Univ. Press, Cambridge

Mandelbrot B.B., 1974, J. Fluid Mech. 62, part 2, 331

Meisenheimer K., Röser H.-J., Schlötelburg M., 1996, A&A 307, 61

Melrose D.B., 1980, Plasma Astrophysics. Gordon and Breach, New York

Menneveau C., Sreenivasan K.R., 1987, Phys. Rev. Lett. 59, 1424

Norman M.L., Hardee P.E., 1988, ApJ 334, 80

Novikov E.A., 1971, Appl. Math. Mech. 35, 231

Novikov E.A., Stewart R.W., 1964, Izvestiya Akademii Nauk SSSR, Seria Geofiz. 3, 408

Parisi G., Frisch U., 1985, On the Singularity Spectrum of Fully Developed Turbulence. In: Ghil M., Benzi R., Parisi G. (eds) Proc. of the International School of Physics "E. Fermi", 1983, Turbulence and Predictability in Geophysical Fluid Dynamics. Varenna, Italy, p. 84

Pacholczyk A.G., 1970, Radio Astrophysics. Freeman, San Francisco

Pelletier G., Zaninetti L., 1984, A&A 136, 313

Pope M.H., Ball L., Melrose D.B., 1996, Publ. Astron. Soc. Aust. 13, 132

Richardson L.F., 1922, Weather Prediction by Numerical Process. Cambridge Univ. Press, Cambridge

Sarris E.T., Van Allen J.A., 1974, J. Geophys. Res. 79, 4157

Scheuer P.A.G., 1984, Adv. Space Res. 4, 337

Schneider P., 1993, A&A 278, 315

Scholer M., 1985, Diffusive Acceleration. In: Tsurutani B.T., Stone R.G. (eds.) Geoph. Mongr. Ser. 35, Collisionless shocks in the Heliosphere: Reviews of Current Research. p. 287

She Z.S., Leveque E., 1994, Phys. Rev. Lett. 72, 336

Tidman D.A., Krall N.A., 1971, Shock Waves in Collisionless Plasmas. Wiley, New York

Van Atta C.W., Yeh T.T., 1973, J. Fluid Mech. 59, 537